J Neurophysiol 97: 2851–2862, 2007.
First published January 31, 2007; doi:10.1152/jn.00860.2006.

Modular Competition Driven by NMDA Receptor Subtypes in Spike-Timing-Dependent Plasticity

Richard C. Gerkin,[1,2,*] Pak-Ming Lau,[3,*] David W. Nauen,[1,2] Yu Tian Wang,[4] and Guo-Qiang Bi[1,2,3]
[1]*Center for Neuroscience and* [2]*Center for the Neural Basis of Cognition, University of Pittsburgh;* [3]*Department of Neurobiology, University of Pittsburgh School of Medicine, Pittsburgh, Pennsylvania; and* [4]*Brain Research Centre and Department of Medicine, University of British Columbia, Vancouver, British Columbia, Canada*

Submitted 14 August 2006; accepted in final form 30 January 2007

Gerkin RC, Lau P-M, Nauen DW, Wang YT, Bi G-Q. Modular competition driven by NMDA receptor subtypes in spike-timing-dependent plasticity. *J Neurophysiol* 97: 2851–2862, 2007. First published January 31, 2007; doi:10.1152/jn.00860.2006. *N*-methyl-D-aspartate receptors (NMDARs) play a critical role in transducing neuronal activity patterns into changes in synaptic strength. However, how they mediate this transduction in response to physiological stimuli has remained elusive. In particular, it has been debated whether different NMDAR subtypes play opposing signaling roles in synaptic plasticity. Using perforated patch-clamp recordings from pairs of synaptically connected glutamatergic neurons in dissociated hippocampal culture, we found that spike-timing-dependent potentiation induced by pairing pre- and postsynaptic spikes required the activation of a fast component of NMDAR current that is likely to be mediated by NR2A-containing NMDARs (NR2A-NRs). In contrast, spike-timing-dependent depression required a slow component of NMDAR current carried by NR2B-containing NMDARs (NR2B-NRs). CV analysis showed that the locus of this depression was primarily presynaptic in pairs of cells making strong synaptic connections, whereas weaker synapses showed no clear preference for pre- or postsynaptic expression. This depression was not significantly reduced by antagonism of the CB1 receptor, in contrast to spike-timing-dependent depression in the neocortex that requires presynaptic CB1 signaling. With blockade of NR2B-NRs, spike triplets that contained both potentiating and depressing spike-timing components induced net potentiation. However, when the putative NR2A-NR population is inhibited, these spike triplets resulted in either depression or no net change, depending on the temporal order of the spike-timing components. These results imply a dynamic competition between signaling modules that can be biased by differentially antagonizing NMDAR subtypes during the induction of spike-timing-dependent plasticity. Using a simple model, we show that such a modular competition recapitulates our observations.

INTRODUCTION

Activity-dependent plasticity shapes neuronal circuits and is proposed to be the cellular substrate of learning and memory (Bliss and Collingridge 1993; Constantine-Paton et al. 1990; Hebb 1949). Because the temporal pattern of action potentials conveys information between neurons, spike-timing-dependent plasticity (STDP) is considered a physiologically relevant and computationally powerful paradigm of activity-induced synaptic modification (Abbott and Nelson 2000; Bi and Poo 2001). In STDP, the timing of action potentials in pre- and postsynaptic neurons is translated into long-term potentiation or long-term depression (LTP or LTD, respectively) of synaptic strength (Bi and Rubin 2005; Dan and Poo 2004). As in conventional paradigms (Malenka and Nicoll 1999), STDP signaling relies on Ca^{2+} influx through *N*-methyl-D-aspartate receptors (NMDARs) (Bi and Rubin 2005; Sjostrom and Nelson 2002). However, it is unclear how NMDARs reliably map the temporal pattern of spikes onto the activation of appropriate downstream targets leading to opposing directions of synaptic modification.

NMDARs containing NR2A and/or NR2B subunits predominate in the mammalian forebrain (Cull-Candy et al. 2001). These subtypes were recently shown to be differentially involved in classical LTP and LTD, respectively (Liu et al. 2004; Massey et al. 2004). However, this picture is complicated by observations using NR2A-knockout mice (Berberich et al. 2005; Weitlauf et al. 2005) and overexpression of NMDAR subunits (Barria and Malinow 2005; Tang et al. 1999), suggesting the existence of NR2A-independent forms of LTP, and by apparently conflicting results published by other investigators (Morishita et al. 2006). Furthermore, it is unknown whether NMDAR subtype specificity can extend to physiological forms of plasticity that involve temporally precise pre- and postsynaptic activity (Bliss and Schoepfer 2004).

To address these issues, we investigated the involvement of NMDAR subtypes in the induction and integration of STDP in paired recordings from cultured hippocampal neurons. We found that NR2A-containing NMDARs (NR2A-NRs) and NR2B-containing NMDARs (NR2B-NRs) made opposing contributions to bidirectional STDP. A fast, NR2A-NR–dominated current was necessary for, and correlated with, spike-timing-dependent potentiation. Meanwhile, NR2B-NR was necessary for spike-timing-dependent depression. This depression, in contrast to spike-timing-dependent depression in the neocortex (Bender et al. 2006; Sjostrom et al. 2003), was not dependent on cannabinoid signaling through the CB1 receptor and its locus could be either pre- or postsynaptic, depending on the developmental stage of the synaptic connection. The effect of spike triplet stimuli, containing multiple pre- or postsynaptic spikes, on synaptic strength depended on which NMDAR subtype was preferentially inhibited. Antagonism of NR2B-NRs unmasked potentiation in an otherwise plasticity-neutral pre-post-pre triplet, whereas antagonism of NR2A-NRs unmasked depression in this triplet and abolished potentiation in a post-pre-post triplet. These results suggest that NMDAR

* These authors contributed equally to this work.

Address for reprint requests and other correspondence: G.-Q. Bi, University of Pittsburgh School of Medicine, Department of Neurobiology, Pittsburgh, PA 15261 (E-mail: gqbi@pitt.edu).

The costs of publication of this article were defrayed in part by the payment of page charges. The article must therefore be hereby marked "*advertisement*" in accordance with 18 U.S.C. Section 1734 solely to indicate this fact.

subtypes can differentially mediate bidirectional STDP in cultured hippocampal neurons.

METHODS

Cell culture and electrophysiology

Low-density cultures of dissociated embryonic rat hippocampal neurons were prepared as previously described (Wang et al. 2005; Wilcox et al. 1994). Hippocampi were removed from embryonic day 18 (E18) to E20 rats and treated with trypsin for 15 min at 37°C, followed by washing and gentle trituration. The dissociated cells were plated at densities of 20,000–50,000 cells/ml on poly-L-lysine–coated glass coverslips in 35-mm petri dishes. The plating medium was DMEM (BioWhittaker, Walkersville, MD) supplemented with 10% heat-inactivated fetal bovine serum (Hyclone, Logan, UT), 10% Ham's F12 with glutamine (BioWhittaker), and 50 U/ml penicillin–streptomycin (Sigma, St. Louis, MO). Twenty-four hours after plating, one third of the culture medium was changed to the above medium containing 20 mM KCl. Both glial and neuronal cell types are present under these culture conditions. At 10–15 days in vitro (DIV), pairs of synaptically connected glutamatergic neurons were recorded using the perforated whole cell patch-clamp technique at room temperature. The pipette solution contained (in mM): K-gluconate 136.5, KCl 17.5, NaCl 9, $MgCl_2$ 1, HEPES 10, EGTA 0.2, and 200 μg/ml amphotericin B (pH 7.3). The external bath solution contained (in mM): NaCl 150, KCl 3, $CaCl_2$ 3, $MgCl_2$ 2, HEPES 10, and glucose 5 (pH 7.3). Signals were acquired using IGOR Pro, MATLAB, or pClamp through a digitizing board (PCI-6035, National Instruments). Recordings showing significant changes (>10%) in series (20–40 MΩ) or input resistance (500–1,500 MΩ) were excluded from further analysis. Only monosynaptic connections between glutamatergic neurons were included in the current study. Polysynaptic currents, identified based on the latency of excitatory postsynaptic current (EPSC) onset (>5 ms), were excluded because their timing could not be precisely controlled. As in previous studies (Wang et al. 2005), connections with strengths only >50 and <500 pA were selected for the NMDAR subtype studies to reduce both heterogeneity in STDP induction and voltage-clamping artifacts. [(*R*)-[(*S*)-1-(4-Bromophenyl)-ethylamino]-(2,3-dioxo-1,2,3,4-tetrahydroquinoxalin-5-yl)-methyl]-phosphonic acid (NVP-AAM077), to preferentially block NR2A-NRs (gift of YP Auberson of Novartis Pharma), or [*R*-(*R**,*S**)]-α-(4-hydroxyphenyl)-β-methyl-4-(phenylmethyl)-1-piperidine propanol (Ro25-6981), to selectively block NR2B-NRs (Sigma), diluted from 1,000 × stock solutions, was perfused into the bath >10 min before the induction of STDP. Addition of either reagent caused no detectable change in the [primarily α-amino-3-hydroxy-5-methyl-4-isoxazolepropionic acid receptor (AMPAR)–mediated] postsynaptic response or in the paired-pulse ratio (50-ms interpulse interval). During STDP induction, the postsynaptic cell (constant current injected to hold at −65 to −70 mV) was in current clamp and stimulation was 1- to 2-nA current injection for 2 ms, sufficient to elicit a spike. Presynaptic stimulation was given by step depolarization (100 mV, 1–2 ms). The neurons were not spontaneously active under recording conditions. Changes in synaptic strength were calculated from the averaged EPSC amplitude 0–10 min before and 15–30 min after the stimulation paradigm.

NMDAR current recording conditions

NMDAR currents were obtained in 10 μM glycine, 0 Mg^{2+}, and 10 μM 6-cyano-7-nitroquinoxaline-2,3-dione (CNQX). NMDAR decay time constants were obtained by fitting single exponentials to the region 40–340 ms after the stimulus. NMDAR current amplitude was defined as the mean current 5–55 ms after presynaptic stimulus onset. As a result of the lesser affinity of glycine for NR2A-NRs versus NR2B-NRs (Kutsuwada et al. 1992), adding a saturating concentration of glycine may enhance NR2A-NR current more than NR2B-NR current, thus overestimating synaptic NR2A-NR currents; furthermore, CNQX can compete with glycine for the glycine-binding site on the NMDAR (Lester et al. 1989). However, the effective concentration of glycine is probably irrelevant because the results reported here do not rely on any specific ratio of NMDAR subtypes. NMDAR currents were also present in the absence of added glycine (data not shown), confirming that glycine site agonists (glycine or D-serine) persist among neurons cocultured with glial cells, as seen previously (Yang et al. 2003). Because the effects of steady-state Mg^{2+} block in NR2A-NRs and NR2B-NRs are indistinguishable (Kuner and Schoepfer 1996; Monyer et al. 1994; Yang et al. 2003), we also assume that recording NMDAR currents in Mg^{2+}-free solution does not bias our measurements toward either of these two subtypes.

Quantification of NMDAR subtype specificity of NVP-AAM077

To estimate the specificity of the competitive antagonist NVP-AAM077 at the concentration we used for our experiments, we recorded synaptic NMDAR currents in pairs of hippocampal neurons in the presence of 10 μM CNQX, 0 Mg^{2+}, and 10 μM glycine. For each experiment, we measured these NMDAR currents as follows: 1) in the absence of NMDAR antagonists (I_{NMDAR}), 2) in the presence of 0.4 μM NVP-AAM077 (I_{NVP}), 3) in the presence of 0.3 μM Ro25-6981 (I_{Ro25}), and 4) in the presence of both 0.4 μM NVP-AAM077 and 0.3 μM Ro25-6981 (I_{Both}), with each step followed by a washout period.

The fraction of Ro25-sensitive current that is blocked by NVP-AAM077 is

$$x = [(I_{NMDAR} - I_{NVP}) - (I_{Ro25} - I_{Both})]/(I_{NMDAR} - I_{Ro25}) \quad (1)$$

Using *Eq. 1* on each of eight different synaptic connections gave a result of x = 35.5 ± 7.6% (median 34.6%), implying that 0.4 μM NVP-AAM077 blocks about one third of the Ro25-sensitive (NR2B-containing) NR current.

The synaptic NMDAR population is likely to contain receptors that possess either NR2A, NR2B, or both NR2 subunits. To analyze this, the fraction of the current carried by NMDARs possessing only NR2A subunits will be denoted *A*, by those possessing only NR2B subunits as *B*, and by those possessing both as $\underline{AB}$. The fractional contribution from any other source (NMDAR or otherwise) providing synaptic current under these conditions will be denoted *Z*. By definition, $A + B + \underline{AB} + Z = 1$. Let us denote the fraction of *A* blocked by NVP-AAM077 as N_A, the fraction of *B* blocked by NVP-AAM077 as N_B, the fraction of $\underline{AB}$ blocked by NVP-AAM077 as N_{AB}, and the fraction of Z blocked by NVP-AAM077 as N_Z, with corresponding variables for the current blocked by Ro25-6981 (R_A, R_B, R_{AB}, and R_Z). Thus *Eq. 1* can also be written as

$$x = \{(N_A A + N_{AB}\underline{AB} + N_B B + N_Z Z) - [N_A A(1 - R_A) + N_{AB}\underline{AB}(1 - R_{AB}) + N_B B(1 - R_B) + N_Z Z(1 - R_Z)]\}/(R_A A + R_{AB}\underline{AB} + R_B B + R_Z Z) = (N_A A R_A + N_{AB}\underline{AB}R_{AB} + N_B B R_B + N_Z Z R_Z)/(A R_A + \underline{AB}R_{AB} + B R_B + Z R_Z) \quad (2)$$

Because of the high selectivity of Ro25-6981, $R_A \simeq 0$, and because each of N_Z, R_Z, and *Z* is likely to be very small, we can approximate

$$x = (N_{AB}\underline{AB}R_{AB} + N_B B R_B)/(\underline{AB}R_{AB} + B R_B) \quad (3)$$

For the extreme cases of $\underline{AB} = 0$ or $B = 0$, $x = N_B$ or $x = N_{AB}$, respectively. Even without assuming these extremes, *Eq. 3* shows that the empirically calculated *x* corresponds to an average of the block by NVP-AAM077 of NR2B–NR2B and NR2A–NR2B subtypes, weighted according to their relative abundance at the synapse and sensitivities to Ro25-6981. Because Ro25-6981 is a more efficacious and selective derivative of ifenprodil, 0.3 μM is likely adequate to antagonize the NR2A–NR2B subtype (see following text) with suffi-

cient efficacy that $R_{AB} \simeq R_B$, implying that x is simply weighted according to the abundance of these subtypes in the synaptic NMDAR population.

We observed that I_{Both} had a slow decay; when fit to a double exponential with the time constants of the Ro25-6981–sensitive (putative NR2B-NR) and –insensitive (putative NR2A-NR) current components, it had a negligible (<1%) contribution from the faster of these two components; thus the block by Ro25-6981 and NVP-AAM077 together effectively abolishes all of the NR2A-NR components. Because the IC_{50} for Ro25-6981 at NR2A-NRs is 52 μM (Fischer et al. 1997), 0.3 μM Ro25-6981 cannot significantly antagonize NR2A-NRs. Therefore 0.4 μM NVP-AAM077 must be sufficient to abolish nearly the entire NR2A-NR component.

Some NMDARs may be NR1–NR2A–NR2B triheteromers with the kinetic properties of NR2B and a sensitivity to ifenprodil-like compounds more reminiscent of NR2B than NR2A (Brimecombe et al. 1997; Hatton and Paoletti 2005; Kew et al. 1998; Neyton and Paoletti 2006). There are no direct studies concerning the ability of NVP-AAM077 to block such receptors. To account for this, *Eq. 3* yields a weighted average of the block of NR2B-NRs and the block of NR2A–NR2B-NRs by NVP-AAM077. However, because NR2A–NR2B-NRs are believed to have slow kinetics similar to those of NR2B-NRs (Vicini et al. 1998), whereas the current blocked by NVP-AAM077 has much more rapid kinetics (Fig. 1, *B* and *C*), the majority of this NVP-AAM077–sensitive current is likely to be mediated by NMDARs containing only the NR2A subunit. NVP-AAM077 can also block NR2C-containing NMDARs (Feng et al. 2004); however, these are believed to be mostly absent in hippocampal principal neurons in vivo (Monyer et al. 1994) and in culture (Janssens and Lesage 2001; Miyashiro et al. 1994; Okada and Corfas 2004). The rapid kinetics of the NVP-AAM077–sensitive NMDAR current also argue against the presence of these kinetically slow NMDAR subtypes.

Modeling

The core model uses four ordinary differential equations (ODEs) inspired by those in Rubin et al. (2005). The variables P, D, and V represent the activation level of signaling modules (enzymatic pathways) activated by Ca^{2+} signals. Instead of tracking the spatiotemporal details of calcium dynamics, the equations are simplified such that each variable increases when a particular spike doublet (combination of pre- and postsynaptic spikes) occurs. In choosing the doublets that would drive the integration of each variable, we observed that *1*) the Ca^{2+} threshold required to achieve potentiation is higher than that required to achieve depression (Bradshaw et al. 2003; Lisman 1989; Shouval et al. 2002; Stemmer and Klee 1994; Yang et al. 1999) and *2*) the *ab* (pre-before-post) doublet provides more calcium influx than the *ba* doublet (Nevian and Sakmann 2004, 2006)

$$P' = ab(t) - p_{off}P \quad (4)$$

$$D' = ba(t) + ab(t) - d_{off}(D + \lambda VD) \quad (5)$$

$$V' = ab(t) - v_{off}V \quad (6)$$

$$W' = 1/\{1 + \exp[(1 - P)/p_{steep}]\} - 1/\{1 + \exp[(1 - D)/d_{steep}]\} - (w_{off}W) \quad (7)$$

Thus P (the potentiation pathway) responds only to the *ab* doublet to reflect this high Ca^{2+} threshold, whereas D (the depression pathway) responds to both the *ab* and *ba* doublets. We chose V to account for the experimental observation that, even when potentiation is pharamacologically blocked, potentiating stimuli are often able to "veto" depressing stimuli, resulting in an absence of depression. Therefore V inhibits D. Last, we assume a simple scheme of modular specificity as illustrated in Fig. 5*A* (solid lines only); thus P can respond only when NR2A-NRs are not inhibited, whereas D and V can respond only when

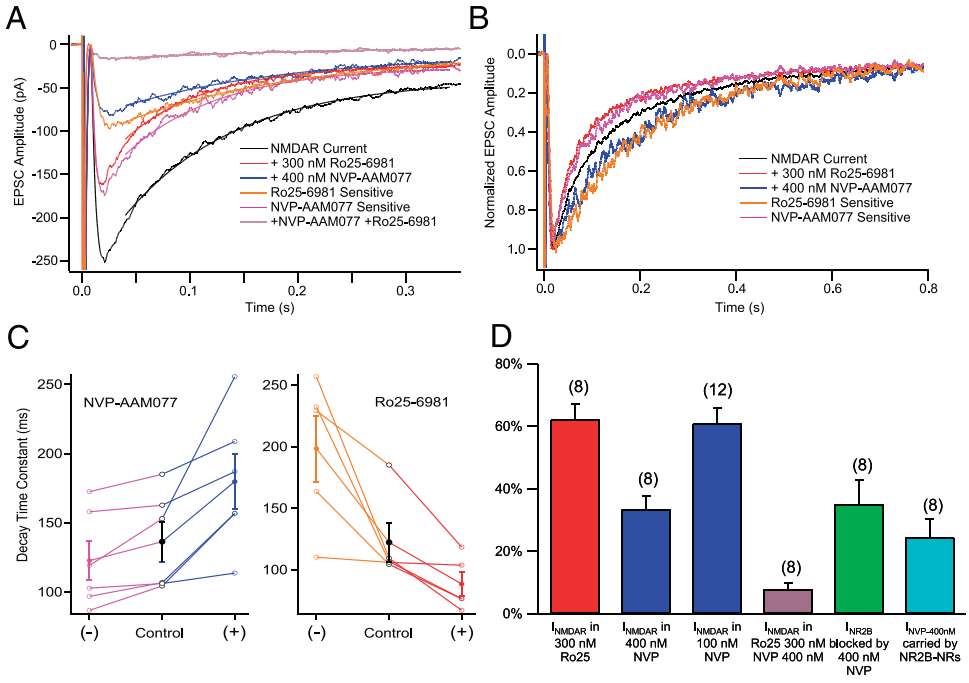

FIG. 1. *N*-methyl-D-aspartate receptor (NMDAR) current amplitudes and kinetics. *A*: example synaptic currents in the presence of 10 μM 6-cyano-7-nitroquinoxaline-2,3-dione (CNQX), 10 μM glycine, and 0 Mg^{2+}. Single-exponential fits are superimposed as solid lines. *B*: traces from *A* normalized and peak-aligned. Trace corresponding to simultaneous presence of both drugs is omitted for clarity. *C1* (*left panel*): NMDAR current decay times in the absence of drugs (*center*), in the presence of 0.4 μM NVP-AAM077 (*right*, +), and the NVP-AAM077–sensitive component (*left*, −) ($n = 5$; $P < 0.05$ for each, paired *t*-test). Filled circles are mean values. *C2* (*right panel*): same as *C1*, except 0.3 μM Ro25-6981 is used ($n = 6$, $P < 0.05$ for each, paired *t*-test). *D*: fraction of NMDAR current remaining in 0.3 μM Ro25-6981; remaining in 0.4 μM NVP-AAM077; remaining in 0.1 μM NVP-AAM077; remaining in both Ro25-6981 and NVP-AAM077; the fraction of NR2B-NR current (Ro25-6981–sensitive) blocked by NVP-AAM077; the NR2B-NR contribution to the current blocked by NVP-AAM077; sample size indicated in parentheses throughout. Error bars are SE.

NR2B-NRs are not inhibited. *ab*(t) and *ba*(t) are transient signals representing the timing of the aforementioned spike doublets. To accord with the experimental protocol, these signals are activated (set equal to 1 for a period of 5 ms) whenever the corresponding spike doublet is present in the STDP induction protocol (once per second); they are equal to zero otherwise. If both the *ab* and *ba* doublets are present (e.g., the *ABA* triplet protocol), they are activated 10 ms apart from one another. *W* reflects a final integration of *P* and *D* and its value reflects the final outcome of an STDP induction (positive = potentiation; negative = depression). The values of the parameters and their descriptions are presented in Table 1. The parameter choices do not require fine-tuning, although large changes in the parameters can lead to different outcomes for triplet experiments (in control conditions), such as those observed in other preparations (Froemke and Dan 2002; Sjostrom et al. 2001). However, our model requires that the kinetics of *V* (represented by v_{off}) must be faster than those of the other modules to reflect the rapid deactivation of the veto module.

Analysis and statistics

Under the assumptions of $1/CV^2$ analysis, the coefficient of variation (CV) for a series of observations of macroscopic postsynaptic current is given by $CV = \sigma/\mu = [np(1 - p)q^2]^{1/2}/npq = (1 - p)^{1/2}/(np)^{1/2}$, where *n* is the number of neurotransmitter release sites, *p* is the probability of release, and *q* is the quantal size. Thus $1/CV^2 = np/(1 - p)$. Under the ideal assumptions, *p* and *q* are identical at every release site; even for the more realistic case where *p* and *q* assume unique values at every site, plasticity corresponding to linear scalings of *n*, *p*, *q*, or any combination of the three, will still secure the conventional interpretation of $1/CV^2$ analysis (Faber and Korn 1991). The CV value was computed by analyzing a segment 0 to 10 min before the STDP induction protocol ("before"), and a segment 15 to 30 min after the STDP induction protocol ("after"). It is assumed that a stationary binomial process governs synaptic transmission at each bouton during each segment. Because the second segment does not necessarily have zero slope, measuring the conventional variance, $E(\mu - x_i)^2$, would overestimate the intrinsic trial-to-trial variance of the synaptic response of this segment and thus give fictive decreases in $(1/CV^2)$ as a result of STDP induction. To address this problem, we subtracted a linear trend from the "before" and "after" segments before measuring the variance. Similar results were obtained by computing the nonstationary variance (Noceti et al. 1996).

Under the same assumptions as those for CV analysis, we define a new measure, the LTD index, calculated from change in synaptic strength divided by change in $1/CV^2$, and is equal to

$$[(n_1p_1q_1)/(n_0p_0q_0)]/\{[n_1p_1/(1 - p_1)]/[n_0p_0/(1 - p_0)]\} = (q_1/q_0)[(1 - p_1)/(1 - p_0)] \quad (8)$$

The subscripts 0 and 1 indicate values before and after STDP induction, respectively. Compared with the unity line in a CV analysis plot (Fig. 3*C*), values of the LTD index >1 represent points below the unity line [putative increases in $(1 - p)$, i.e., likely presynaptic changes] and values <1 represent points above the line (putative decreases in *q*, i.e., likely postsynaptic changes). The LTD index has the advantage of condensing the changes in pre- and/or postsynaptic efficacy into a single number, such that decreases in *p*, *n*, and *q* lead to LTD indices >1, =1, and <1, respectively. Its interpretation involves the same assumptions made in conventional $1/CV^2$ analysis as discussed above. Because the a priori distributions of both $1/CV^2$ and the LTD index (see RESULTS) are centered at 1 and are log-normal (a value of 2 is as likely as a value of 0.5), logarithmic axes and transformations are used in Fig. 3, *C* and *D*. A Student's *t*-test was used for all statistical comparisons unless otherwise indicated. A Bonferroni correction for multiple comparisons to the same control was made where applicable. Comparisons to unity (100%, no change in synaptic strength) remain uncorrected. Values are reported as means ± SE.

TABLE 1. *Parameters for the model simulated in Fig. 5*

Parameter	Description	Value
p_{off}	The rate at which the activation of the potentiation pathway *P* decays	1/30
d_{off}	The rate at which the activation of the depression pathway *D* decays	1/30
v_{off}	The rate at which the activation of the "veto" pathway *V* decays	1
w_{off}	The rate at which the final readout *W* decays	1/3000
λ	The effect of the "veto" pathway *V* on the depression pathway *D*	1,000
p_{steep}	The sensitivity of *W* to the activation of *P*	1/5
d_{steep}	The sensitivity of *W* to the activation of *D*	1/5

RESULTS

NMDAR subtypes in cultured hippocampal neurons

Previous studies on the roles of NMDAR subtypes in synaptic plasticity used Ro25-6981, which specifically blocks NR2B-NRs (Fischer et al. 1997), and NVP-AAM077, which preferentially inhibits NR2A-NRs (Berberich et al. 2005; Feng et al. 2004; Liu et al. 2004; Weitlauf et al. 2005). However, the use of pharamacological agents to dissect NMDAR subtype contributions has also been criticized, especially because of the disputed selectivity of NVP-AAM077 (Neyton and Paoletti 2006). Because NVP-AAM077 is a competitive antagonist, the effective receptor block will be a function of the magnitude and dynamics of glutamate concentration in the cleft, which are not accurately replicated using iontophoresis. Therefore direct application of glutamate cannot be used as a proxy to determine the effect of NVP-AAM077 on responses induced by synaptic activity. We examined the existence of distinct NMDAR subtypes and tested NVP-AAM077 directly on synaptic transmission in our system, thus ensuring that the relevant temporal profile of glutamate was used to make this measurement. To evaluate the effect of antagonists to synaptic NMDAR currents, we identified pairs of glutamatergic neurons by intracellular stimulation and recorded evoked synaptic currents in one neuron in response to stimulation of its presynaptic partner in the presence of 10 μM CNQX, 0 Mg^{2+}, and 10 μM glycine. Either 0.3 μM Ro25-6981 or 0.4 μM NVP-AAM077 was then added to the bath to assess the effect of these reagents on the NMDAR current (Fig. 1, *A* and *B*). Ro25-6981 caused a 37.9 ± 5.1% decrease in the magnitude of the NMDAR current (Fig. 1*D*) and a decrease in the average decay time of the current (see METHODS) from 122.3 ± 15.7 to 88.5 ± 9.7 ms (means ± SE, $P < 0.05$ by a paired *t*-test, Fig. 1*C1*), suggesting the predominance of a rapidly decaying NR2A-NR component in the remaining current. In contrast, application of NVP-AAM077 caused a decrease in the magnitude of the NMDAR current of 65.6 ± 4.3% (Fig. 1*D*), but an increase in the decay time from 136.3 ± 14.3 to 179.7 ± 20.0 ms ($P < 0.05$ by a paired *t*-test, Fig. 1*C2*), indicating a mostly slow NR2B-NR component in the remaining current. Because 0.4 μM NVP-AAM077 was also previously shown to block a fraction of NR2B-NR current in heterologous expression systems and in NR2A-NR knockout animals (Berberich et al. 2005; Weitlauf et al. 2005), we determined its specificity in our preparation. Based on synaptic NMDAR currents in the presence of either,

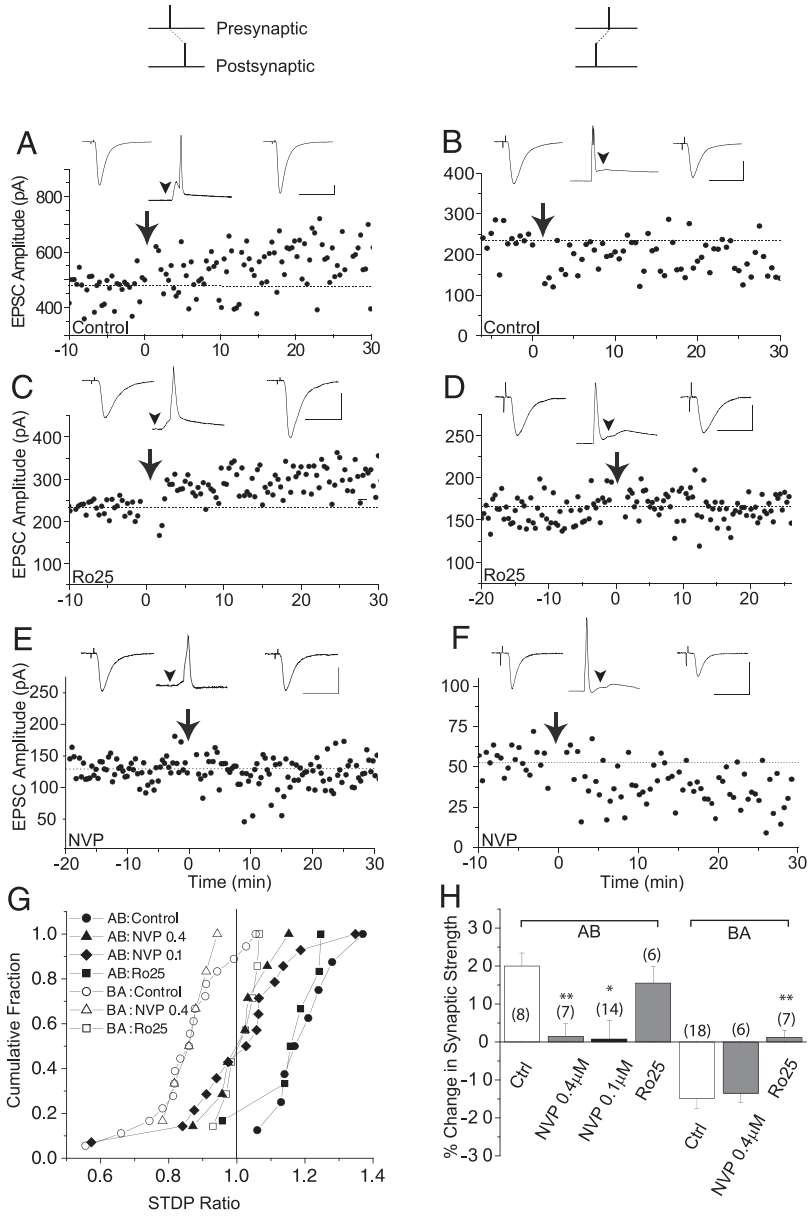

FIG. 2. Spike-timing-dependent potentiation specifically requires non-NR2B-NRs (putative NR2A-NRs), whereas spike-timing-dependent depression specifically requires NR2B-NRs. *A*: potentiation is induced by positive spike timing ($\Delta t = +8$ ms). *B*: depression is induced by negative spike timing ($\Delta t = -8$ ms). *C*: potentiation induced by positive spike timing persists in the presence of 0.3 μM Ro25-6981. *D*: negative spike timing fails to induce depression in the presence of Ro25-6981. *E*: positive spike timing fails to induce potentiation in the presence of 0.4 μM NVP-AAM077. *F*: depression induced by negative spike timing remains intact in the presence of 0.4 μM NVP-AAM077. *G*: cumulative histogram of experiments with spike pairs. *AB*, pre-post spike pairs; *BA*, post-pre spike pairs. *H*: change in synaptic strength for all experiments with spike pairs (means $\pm$ SE). * indicates $P < 0.05$ vs. corresponding controls; ** indicates $P < 0.01$ (Student's *t*-test). *AB* control vs. *AB* Ro25-6981: $P = 0.56$; *BA* control vs. *BA* 0.4 μM NVP-AAM077: $P = 0.80$. *Insets*: example traces from the postsynaptic cell before (*left*), during (*middle*) and after (*right*) STDP induction; arrowheads indicate presynaptic cell stimulation. Scale bars: 20 ms, 100 pA (voltage clamp). Autaptic excitatory postsynaptic potentials (EPSPs) in the postsynaptic cell are visible in some insets.

neither, or both 0.4 μM NVP-AAM077 and 0.3 μM Ro25-6981 (see METHODS), we estimated that 0.4 μM NVP-AAAM077 blocked nearly all of the Ro25-6981–insensitive current (non-NR2B-NR current) as well as roughly one third (35.5 $\pm$ 7.6%) of the Ro25-6981–sensitive current (NR2B-NR current, Fig. 1*D*).

Thus the apparent specificity of NVP-AAM077 in response to synaptically released glutamate our system is less than that previously observed for oocyte-expressed human NMDARs and wild-type rat hippocampal slices (Liu et al. 2004), but greater than that observed for rodent NMDARs expressed in HEK cells or in hippocampal neurons from NR2A knockout mice (Berberich et al. 2005; Weitlauf et al. 2005). Differences in the expression of triheteromeric NMDARs (see METHODS) as well as variations in glutamate concentration across these preparations and thus in the ability of NVP-AAM077 to outcompete glutamate at each NMDAR subtype may be partly responsible for the inconsistency of the literature. Because NVP-AAM077 and Ro25-6981 reveal NMDAR subpopulations with vastly different kinetics and because NR1–NR2A–NR2B triheteromers have kinetic and pharmacological properties similar to those of NR1–NR2B–NR2B-NRs (Hatton and Paoletti 2005; Vicini et al. 1998), for simplicity we will refer to the Ro25-6981–sensitive subpopulation with slow kinetics as NR2B-NRs and the NVP-AAM077–sensitive subpopulation with fast kinetics as NR2A-NRs.

Roles of NMDAR subtypes in the induction of bidirectional STDP

To study the roles of NMDAR subtypes in STDP, dual perforated voltage-clamp recordings were performed in the presence of either Ro25-6981 or NVP-AAM077. After obtaining a 10- to 15-min baseline of synaptic responses, a spike-timing-dependent pairing protocol was delivered (1-Hz stimulation for 60 s with the postsynaptic cell in current clamp; spike timing Δt was between 8 and 10 ms for "pre-post" and between -8 and -10 ms for "post-pre" spike pairs) to induce spike-

timing-dependent LTP or LTD. We confirmed that under control conditions, as in previous studies using this system (Bi and Poo 1998; Wang et al. 2005), pre-post (*AB*) spike pairing resulted in synaptic potentiation (Fig. 2, *A*, *G*, and *H*; 120.6 ± 3.8%, $n = 8$, $P < 0.001$ vs. unity), whereas post-pre (*BA*) spike pairing resulted in synaptic depression (Fig. 2, *B*, *G*, and *H*; 85.1 ± 2.9%, $n = 18$, $P < 0.001$ vs. unity). Blockade of NR2B-NRs with Ro25-6981 had no significant effect on spike-timing-dependent potentiation (Fig. 2, *C*, *G*, and *H*; 115.5 ± 4.3%, $n = 6$, $P < 0.05$ vs. unity, $P > 0.3$ vs. control), but abolished spike-timing-dependent depression (Fig. 2, *D*, *G*, and *H*; 101.2 ± 2.0%, $n = 7$, $P > 0.5$ vs. unity, $P < 0.01$ vs. control), indicating that NR2B-NRs are required for spike-timing-dependent depression but not for potentiation.

In contrast, addition of the NR2A-preferring antagonist NVP-AAM077 (0.4 μM) prevented the synaptic potentiation typically induced by pre-post spike pairs (Fig. 2, *E*, *G*, and *H*; 101.4 ± 3.5%, $n = 7$, $P > 0.5$ vs. unity, $P < 0.01$ vs. control) without significantly altering the synaptic depression induced by post-pre spike pairs (Fig. 2, *F*, *G*, and *H*; 86.5 ± 2.4%, $n = 6$, $P < 0.005$ vs. unity, $P > 0.5$ vs. control), arguing for a requirement of NR2A-NR activation in spike-timing-dependent potentiation but not depression. Because 0.4 μM NVP-AAM077 blocks more NMDAR current than does 0.3 μM Ro25-6981, the possibility existed that the magnitude of the remaining NMDAR current, rather than the subtype mediating it, led to abolition of LTP in NVP-AAM077 but not in Ro25-6981. To test this possibility, we repeated the LTP experiments in 0.1 μM NVP-AAM077, a concentration that blocks a similar amount of NMDAR current as 0.3 μM Ro25-6981 (37.9 ± 5.1% for 0.3 μM Ro25-6981, $n = 8$; 39.2 ± 5.1% for 0.1 μM NVP-AAM077, $n = 12$; $P > 0.4$, Fig. 1*D*; see also Supplementary Fig. S1).[1] LTP was still absent under this condition (Fig. 2, *G* and *H*; 100.8 ± 4.8%, $n = 14$, $P < 0.01$ vs. control, $P < 0.05$ vs. LTP in 0.3 μM Ro25-6981, $P > 0.5$ vs. unity). Therefore in response to pairs of pre- and postsynaptic spikes, a unitary synaptic connection (the net monosynaptic connection between two recorded cells) is capable of generating either NR2B-independent (and likely NR2A-dependent) potentiation or NR2B-dependent depression in a manner determined only by the timing of individual action potentials. This evidence suggests that the induction of STDP is mediated by distinct functional modules, with an NMDAR subpopulation containing the NR2A subunit preferentially driving the potentiation module and NR2B-NRs driving the depression module.

The cannabinoid receptor CB1 was previously implicated in spike-timing-dependent depression, but not potentiation, in cortical neurons (Bender et al. 2006; Sjostrom et al. 2003). It was proposed that CB1 receptors located on presynaptic terminals receive a timing-dependent retrograde signal from activated postsynaptic neurons, which coordinates with the activation of presynaptic NR2B-NRs to produce depression (Sjostrom et al. 2003). Because spike-timing-dependent depression in our system also required activation of NR2B-NRs (although the locus of these NR2B-NRs is unidentified) it is of interest to examine whether CB1 signaling plays a role here. In the presence of the CB1 antagonist *N*-(piperidin-1-yl)-5-(4-iodophenyl)-1-(2,4-dichlorophenyl)-4-methyl-1H-pyrazole-3-car-

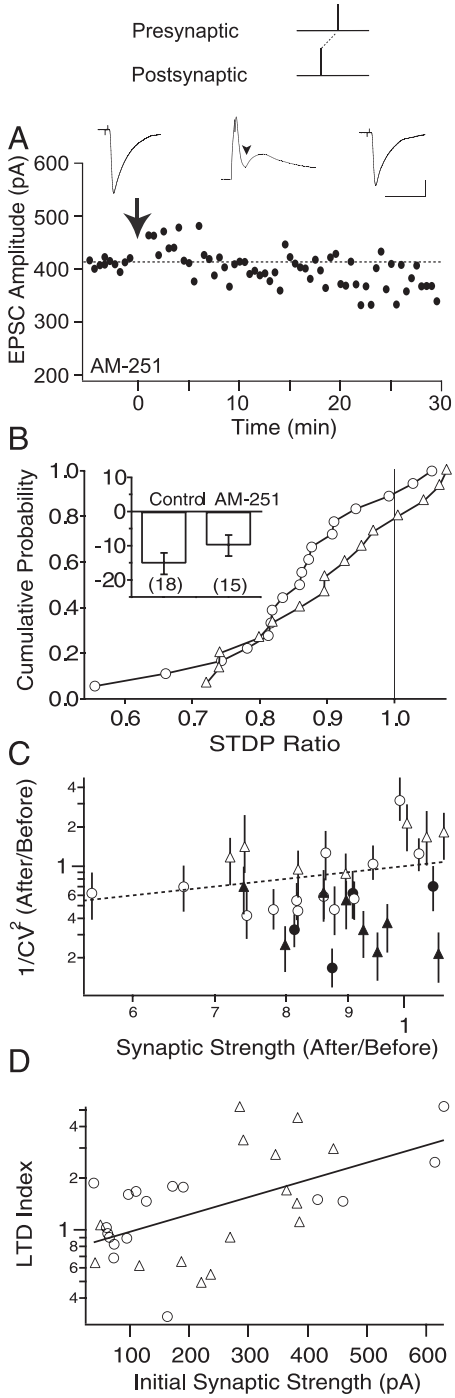

FIG. 3. CB1 antagonism does not block hippocampal spike-timing-dependent depression. *A*: example showing spike-timing-dependent long-term depression (LTD) in the presence of *N*-(piperidin-1-yl)-5-(4-iodophenyl)-1-(2,4-dichlorophenyl)-4-methyl-1H-pyrazole-3-carboxamide (AM-251). *B*: cumulative histogram of experiments using 1–2 μM AM-251 compared with controls. *Inset*: percentage change in synaptic strength for each condition. *C*: coefficient of variation (CV) analysis shows that only strong synaptic connections have a consistently presynaptic locus. Open symbols are weak connections; filled symbols are strong connections (see text). Error bars indicate SE of the $1/CV^2$ measurement. *D*: correlation between the LTD index (ratio between the multiplicative changes in synaptic strength and $1/CV^2$; see METHODS) and the initial synaptic strength ($r = 0.54$, $P < 0.0005$ for the null hypothesis of no correlation). This correlation suggests that strong unitary connections are more likely than weak connections to show increased failure rate ($1 - p$), rather than decreased quantal size (q), after LTD induction. In *B–D*, circles are control experiments; triangles are experiments done in AM-251. Insets, arrowheads, and scale bars are as in Fig. 2.

[1] The online version of this article contains supplemental data.

boxamide (AM-251, 1–2 μM; Sigma), we attempted to induce LTD using "post-pre" spike pairs ($\Delta t = -8$ to -10 ms) (Fig. 3*A*). LTD resulted (Fig. 3*B*; 90.0 ± 3.1%, $n = 15$, $P < 0.005$ vs. unity) and, although it appeared to be less pronounced than that under control conditions, this difference was not significant (control: 85.2 ± 2.9%, $n = 18$, $P < 0.0001$ vs. unity, $P > 0.25$ for AM-251 vs. control). This suggests that CB1 signaling does not contribute significantly to spike-timing-dependent depression in hippocampal neurons. Although this LTD did not require the putative retrograde messenger pharamacology observed in cortical timing-dependent LTD, we wondered whether the locus of spike-timing-dependent LTD could still be presynaptic (Bender et al. 2006; Sjostrom et al. 2003). Indeed, we found a modest increase in paired-pulse ratio (PPR) after post-pre spike pairs in both AM-251 and in control conditions (PPR, after vs. before: 112.8 ± 6.3% in control, $n = 9$, $P < 0.1$ vs. unity; 109.8 ± 3.6% in AM-251, $n = 15$, $P < 0.01$ vs. unity), suggesting possible involvement of presynaptic mechanisms. Because recent studies suggested that paired-pulse facilitation can have postsynaptic origins (Bagal et al. 2005), we also performed a $1/CV^2$ analysis. This analysis compares the change in the coefficient of variation to the change in the mean synaptic response as a result of plasticity induction (Faber and Korn 1991). Changes in release probability (p) are reflected by greater changes in $1/CV^2$ than in mean strength, whereas the reverse is true for changes in quantal size (q). This analysis appeared to show great heterogeneity of LTD locus (Fig. 3*C*). We then reasoned that the locus of LTD might change with synaptic development, as previously observed for LTP (Palmer et al. 2004). Thus we subdivided the experiments into those with high initial unitary connection strengths (the largest dozen connections, 416.9 ± 31.6 pA, $n = 12$, HIGH) and those with low unitary connection strengths (the remaining connections, 122.3 ± 15 pA, $n = 20$, LOW). Although the LOW group still showed no consistent locus of LTD (Fig. 3*C*, open symbols, 8/20 points below the unity line, $P > 0.25$), the HIGH group showed a consistent presynaptic locus (Fig. 3*C*, closed symbols, 12/12 points below the unity line, $P < 0.001$). These data indicate that the expression of spike-timing-dependent LTD has a more consistent presynaptic locus in strong unitary connections. This may reflect a shift toward a presynaptic locus for LTD during synaptic maturation.

Given the quantal assumptions of $1/CV^2$ analysis, algebraic rearrangement (see METHODS) shows that the fractional change in mean synaptic strength divided by the fractional change in $1/CV^2$ is equal to the fractional change in quantal size times the fractional change in the failure rate: $(q_{after}/q_{before}) \times [(1 - p_{after})/(1 - p_{before})]$. Therefore this product, referred to here as the *LTD index*, should be <1 when LTD is mostly postsynaptic and >1 when LTD is mostly presynaptic. This index is thus an alternative representation of the information provided by a $1/CV^2$ analysis of the data. As shown in Fig. 3*D*, we found that the LTD index is strongly positively correlated with initial synaptic strength ($r = 0.70$, $P < 0.001$ for control; $r = 0.50$, $P < 0.05$ for AM-251; $r = 0.54$, $P < 0.0005$ for pooled data; highlighting a tendency toward presynaptic LTD in stronger connections. These results suggest that at least in strong synapses, retrograde signaling mechanisms other than the endocannabinoid/CB1 system are responsible for the spike-timing-dependent LTD in hippocampal neurons. It should be noted that as with classical CV analysis, interpretation of the LTD index relies on a set of basic assumptions regarding synaptic properties (see METHODS) and may be invalid when pre- or postsynaptic changes are nonuniform across boutons.

Integration of NMDAR-subtype–mediated STDP

Neuronal activity in vivo involves ongoing complex spike patterns that contain both positive and negative spike timings, with the final plasticity outcome following second-order rules of STDP integration (Bi and Rubin 2005; Froemke and Dan 2002; Sjostrom and Nelson 2002; Wang et al. 2005). The simplest paradigm for such integration involves spike triplets, with two spikes in one neuron temporally bisected by one spike in the other neuron. Thus each triplet consists of both pre-post and post-pre spike-pairing doublets. The spike-timing interval for each doublet was chosen to be 8–10 ms, for consistency with the spike-pair experiments. As in previous studies using cultured hippocampal neurons (Wang et al. 2005), the pre-post-pre (*ABA*) triplet led to apparent cancellation of potentiation and depression with no net change in synaptic strength (Fig. 4, *A*, *G*, and *H*; 100.2 ± 2.7%, $n = 5$, $P > 0.4$ vs. unity), whereas the post-pre-post (*BAB*) triplet yielded potentiation (Fig. 4, *B*, *G*, and *H*; 121.0 ± 2.5%, $n = 5$, $P < 0.005$ vs. unity). These results are also seen in spike quadruplets and are independent of the paired-pulse ratio of the synaptic connection. However, in the presence of Ro25-6981, the *ABA* triplet induced potentiation of synaptic strength (Fig. 4, *C*, *G*, and *H*; 115.6 ± 1.7%, $n = 5$, $P < 0.001$ vs. unity, $P < 0.005$ vs. control), suggesting that blocking NR2B-NRs unmasks potentiation. On the other hand, Ro25-6981 had no significant effect on the synaptic potentiation produced by the *BAB* triplet (Fig. 4, *D*, *G*, and *H*; 119.6 ± 3.5%, $n = 6$, $P < 0.005$ vs. unity, $P > 0.5$ vs. control).

In the presence of NVP-AAM077, the *ABA* triplet produced synaptic depression (Fig. 4, *E*, *G*, and *H*; 87.5 ± 2.3%, $n = 10$, $P < 0.001$ vs. unity, $P < 0.05$ vs. control), highlighting that preferentially blocking NR2A-NRs unmasks depression in this condition. These results are consistent with the idea that the timing of spikes in the *ABA* triplet normally leads to the concomitant activation and subsequent cancellation of both the NVP-AAM077–sensitive potentiation and Ro25-6981–sensitive depression modules. However, for the *BAB* triplet stimulation protocol, we found that NVP-AAM077 did not unmask depression, but rather resulted in no net change in synaptic strength (Fig. 4, *F*, *G*, and *H*; 100.1 ± 5.0%, $n = 9$, $P > 0.5$ vs. unity, $P < 0.05$ vs. control), suggesting that the depression module failed to activate in response to this spike-timing pattern and was possibly suppressed by an unidentified "veto" module. Such a veto would involve the specific suppression of the depression pathway in response to potentiating stimuli (see following text). These results from triplet experiments show that a single protocol can yield potentiation or depression (or no change), depending only on the availability of NMDAR subtypes.

Dynamic competition of signaling modules

These findings demonstrate that NMDAR subtypes differentially activate competitive signaling modules in the induction and integration of STDP. They complement our previous observations supporting modularity through downstream ki-

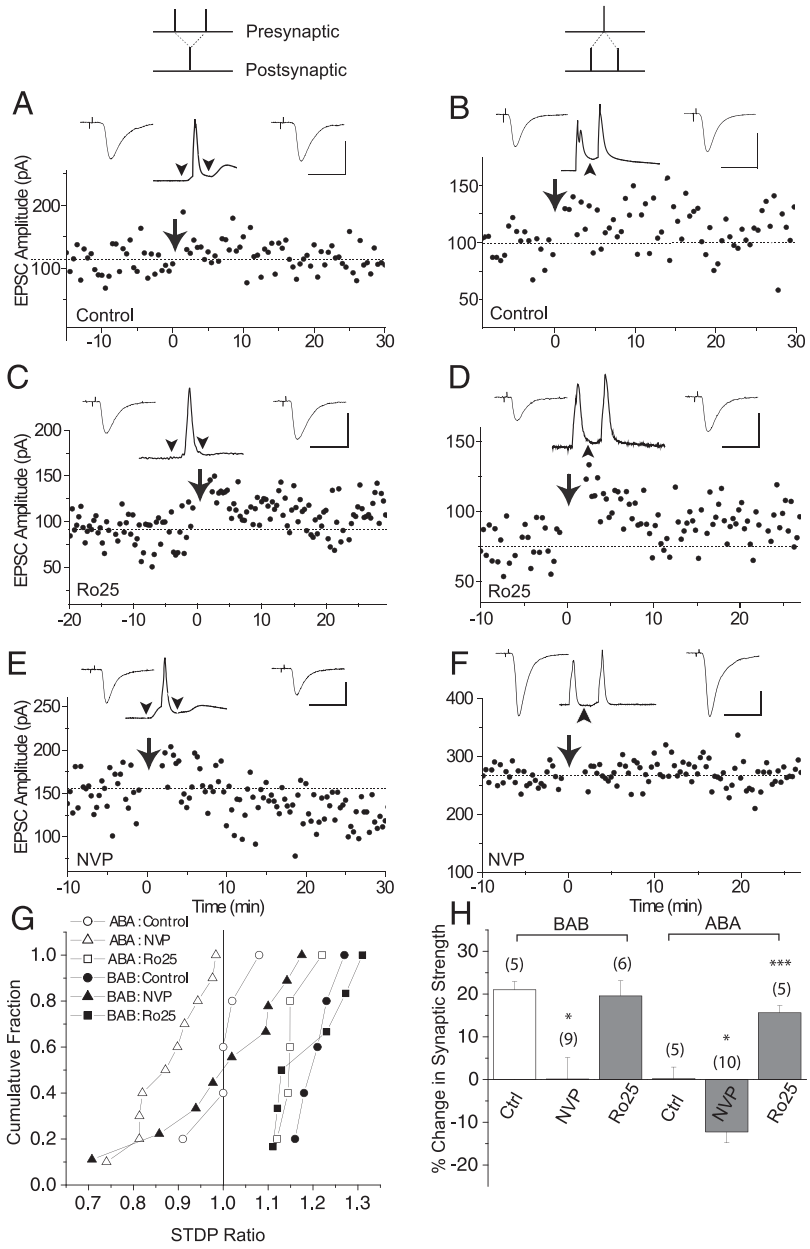

FIG. 4. Triplet experiments show that potentiation is unmasked by antagonizing NR2B-NRs, whereas either depression is unmasked or potentiation is abolished by antagonizing NR2A-NRs. *A*: *ABA* triplet causes no net change in synaptic strength ($\Delta t = +8$ ms, -8 ms). *B*: *BAB* triplet causes synaptic potentiation ($\Delta t = -8$ ms, $+8$ ms). *C*: potentiation is unmasked in the *ABA* triplet in the presence of 0.3 μM Ro25-6981. *D*: potentiation persists in the *BAB* triplet in the presence of Ro25-6981. *E*: depression is unmasked in the *ABA* triplet in the presence of 0.4 μM NVP-AAM077. *F*: *BAB* triplet yields no net change in synaptic strength in the presence of 0.4 μM NVP-AAM077. *G*: cumulative histogram of all experiments with spike triplets. *H*: change in synaptic strength for all experiments with spike triplets (means $\pm$ SE). $^*P < 0.05$ vs. corresponding controls; $^{***}P < 0.005$ (Student's *t*-test). Insets, arrowheads, and scale bars are as in Fig. 2.

nases and phosphatases (Wang et al. 2005). Together, these results indicate that the activity of specific NMDARs is closely tied to the activation of specific enzymes. In particular, they suggest that a subpopulation of NMDARs, whose fast kinetics and NVP-AAM077 sensitivity implicate the NR2A subunit, may drive the activation of calmodulin-dependent protein kinase II (CaMKII) leading to synaptic potentiation. They also suggest that the activation of an NR2B-containing NMDAR subpopulation coordinates with calcineurin (CaN) to produce depression (Fig. 5*A*).

To investigate the possibility of a veto module, we extended (see METHODS) a simplified version of a rigorous model (Rubin et al. 2005) to reflect NR2 subunit specificity. Because pre-post spike pairings yield higher levels of Ca^{2+} influx than post-pre spike pairings (Nevian and Sakmann 2004), these two spike doublets should be readily distinguishable by Ca^{2+}-sensitive machinery (e.g., CaMKII, CaN) in the postsynaptic density. Thus we provide the timing of these doublets directly as inputs to our model. The model consists of three dynamic elements: a potentiation module *P* (by analogy to CaMKII), activated by Ca^{2+} influx through Ro25-insensitive (putative NR2A-containing) NMDARs, as well as a depression module *D* (by analogy to the calcineurin/PP1 system) and a rapidly inactivating veto module *V* (corresponding to an unidentified kinase or other signaling enzyme), both of which are activated by Ca^{2+} influx through NR2B-NRs. *P* and *D* are integrated to give *W*, which relates to the consequent change in synaptic strength. Consistent with the Ca^{2+} threshold being greater for synaptic potentiation than depression (Lisman 1989; Shouval et al. 2002; Yang et al. 1999) and the affinity of CaMKII for Ca^{2+}/calmodulin being lower than that of CaN/PP1 (Bradshaw et al. 2003; Stemmer and Klee 1994), *P* and *V* respond only to pre-post spike doublets, whereas *D* responds to both pre-post and post-pre spike doublets. The purpose of *V* is to allow large-amplitude Ca^{2+} influx (evoked by pre-post dou-

blets) to negate the activation of *D* under appropriate spike-timing conditions, thus accounting for our experimental observations.

In this model, perfect antagonism of the putative NR2A-NR pathway corresponds to a silencing of *P*. However, the pre-post doublet can still activate *V* through NR2B-NRs; if this occurs immediately after *D* has been activated (e.g., post-pre-post triplet), *D* will be silenced by the transient *V*. In contrast, perfect antagonism of NR2B-NRs allows only *P* to be activated. *P* responds only to the pre-post doublet, yielding potentiation. This model makes quantitative predictions that agree with our experimental findings (Fig. 5*B*). Furthermore, it is in agreement with the results of our previous work on the integration of STDP (Wang et al. 2005). The veto also helps explain more generally why LTP stimuli often do not yield LTD when LTP pathways are blocked, despite putatively sufficient Ca^{2+} influx; for example, LTD is not observed in the presence of NVP-AAM077 in response to high-frequency stimulation (HFS) (Liu et al. 2004). However, because NVP-AAM077 is not perfectly selective for NR2A-NRs, we also simulated the model using the levels of antagonism of the NR2A-NR and NR2B-NR components found experimentally (see METHODS, RESULTS) for NVP-AAM077 (Fig. 5*C*). Because of the modular competition inherent in the model, it proved robust to this imperfect selectivity and LTD was preserved as in the experimental data.

We also suspected that if NR2A-NRs were responsible for spike-timing-dependent LTP, this LTP might be correlated with the abundance of NR2A-NRs. To test this, we measured the magnitude (see METHODS) of NMDAR currents 30 min after STDP induction. In accordance with a role for NR2A-NRs in spike-timing-dependent LTP, the potentiation observed in the presence of Ro25-6981 was proportional (least-squares linear regression, $r = 0.84$, $P < 0.01$) to the relative abundance of the putative NR2A-NR current (NMDAR current in the presence of Ro25-6981 normalized to AMPAR current amplitude in the absence of drugs and in normal Mg^{2+} at the same synaptic connection; Fig. 5*D*, red). Using a multiple linear regression model (Table 2), we found that this correlation was not explained by the dependency of STDP on initial synaptic strength

TABLE 2. *ANOVA table from a multiple linear regression using the covariates NR2A-NR abundance and initial synaptic strength to predict the percentage change in synaptic strength*

Parameter	Value	Error	*t*-Value	*P*-Value
Intercept, %	−4.49	6.77	−0.66	0.54
NR2A abundance	134.4	30.3	4.43	0.007
Initial strength, pA	0.035	0.017	2.07	0.09

The table shows that the correlation between NR2A-NR abundance (defined in the main text) and percentage change in synaptic strength cannot be explained by initial synaptic strength.

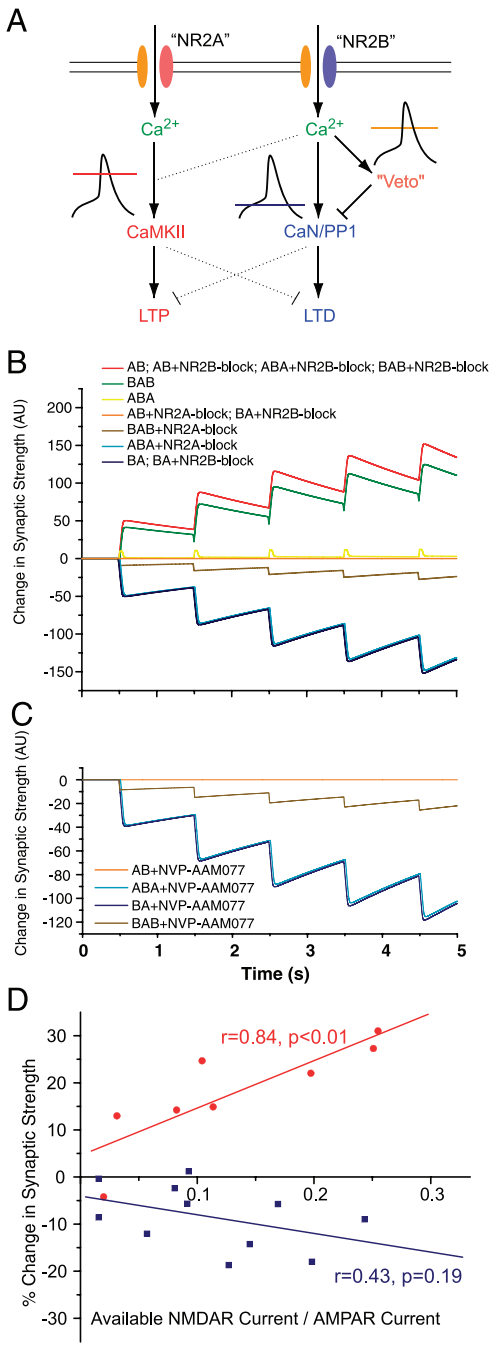

FIG. 5. A dynamic, modular competition among distinct plasticity elements captures the NMDAR subtype and stimulus specificity of spike-timing-dependent plasticity (STDP). *A*: schematic representation of the proposed pathways for the transduction of STDP. In this model, putative NR2A- and NR2B-containing NMDARs are proposed to lie on the postsynaptic membrane, although presynaptic NMDARs have not been definitively excluded. Solid black curves depict Ca^{2+} transients. Horizontal lines depict thresholds of Ca^{2+} influx necessary to activate each module. Dotted lines indicate potential competitive relationships between the potentiation and depression modules. *B*: results from a simple simulation (see METHODS) corresponding to the schematic representation, where *AB* refers to pre-post spike pairs, *BA* refers to post-pre spike pairs, *ABA* refers to pre-post-pre spike triplets, and *BAB* refers to post-pre-post spike triplets. In the simulation, correlated spiking is repeated 5 times at 1 Hz. "Plasticity readout" corresponds to the variable *W* in the model, an indicator related to the magnitude of final synaptic modification. Results from correlated spiking repeated 60 times continue the same trend and are omitted for clarity. *C*: results obtained for block by 0.4 μM NVP-AAM077, assuming that in addition to blocking NR2A-NRs, it blocks one third of the current from NR2B-NRs, as reported in Fig. 1. *D*: long-term potentiation (LTP) observed in the presence of Ro25-6981 induced by protocols with "pre-post" spike doublets is plotted (red) against putative NR2A-NR abundance [NMDAR current in the presence of Ro25-6981 normalized by α-amino-3-hydroxy-5-methyl-4-isoxazolepropionic acid receptor (AMPAR) current]. LTD observed in the presence of NVP-AAM077 induced by protocols with "post-pre" doublets is plotted (blue) against the relative abundance of NR2B-NRs. (NMDAR current blocked by Ro25-6981 normalized by AMPAR current.)

(Bi and Poo 1998). Thus it appears that potentiation depends quantitatively on the relative level of functional NR2A-NR expression in the synaptic population. No statistically significant correlation was observed ($r = -0.43$, $P = 0.19$) between the relative abundance of NR2B-NRs (as measured by the fraction of NMDAR current blocked by Ro25-6981, normalized to AMPAR current) and synaptic depression (Fig. 5*D*, blue).

DISCUSSION

In this study, we show that for spike-timing-dependent plasticity, two subpopulations of NMDARs preferentially mediate the activation of distinct functional modules. Together with other recent findings (Wang et al. 2005; Zhou et al. 2005), these results suggest that STDP cannot be explained by the classical picture wherein the overall level of postsynaptic Ca^{2+} alone determines the plasticity outcome (Artola and Singer 1993). Superficially, the basic results of STDP appear to be consistent with the classical "calcium hypothesis" because the Ca^{2+} influx through NMDARs is greater for *AB* stimuli than for *BA* stimuli (Nevian and Sakmann 2004). However, reducing Ca^{2+} influx with Ro25-6981 in the otherwise plasticity-neutral *ABA* condition actually unmasked LTP (Fig. 4, *A*, *E*, and *F*). Furthermore, whereas partial reduction of Ca^{2+} influx with Ro25-6981 abolished depression in the post-pre spike pairing (*BA*) (Fig. 2, *B*, *E*, and *F*), a greater reduction by NVP-AAM077 (Fig. 1*D*) did not compromise depression (Fig. 2, *D*, *E*, and *F*). These nonlinearities are best explained by the existence of NMDAR-subtype–sensitive potentiation and depression modules, the dynamic competition of which determines the outcome of STDP.

Interestingly, the *AB* and *BAB* stimuli failed to produce depression in the presence of NVP-AAM077, despite Ca^{2+} influx putatively sufficient, as indicated by the success of *BA* under the same conditions, to activate the depression module. One possibility is that the NR2B-NR–mediated, CaN-dependent depression module is actively suppressed ("vetoed") in a spike-timing-dependent fashion by a module that is not of itself potentiation. This veto would be activated by strong Ca^{2+} transients but NVP-AAM077 insensitive (i.e., Ca^{2+} influx through NR2B-NRs would be sufficient). Indeed, a previous modeling study (Rubin et al. 2005) predicted that a calcium-triggered "veto" was necessary to reconcile STDP outcomes with known Ca^{2+} dynamics. We extended this by separating NMDAR-mediated Ca^{2+} influx into distinct pools, so that the current model (Fig. 5, *B* and *C*) matches experimental outcomes with fewer dynamical equations and without fine-tuning of parameters. It is noted that, although not considered in our model, there may also be a role for the stochasticity of vesicle release in explaining the observed results (Cai et al. 2006; Shouval and Kalantzis 2005).

A crucial issue in this and related studies has been the specificity of antagonists (Neyton and Paoletti 2006). We showed that 0.4 μm NVP-AAM077 blocked roughly one third of the synaptic NR2B-NR currents in our preparation. This analysis, based on measurements using 0.033-Hz stimuli, may overestimate the "nonspecific" blockade of NR2B-NRs by NVP-AAM077 during STDP paradigms ($\geq$1-Hz presynaptic stimulation) because the NR2B-NR inhibition by NVP-AAM077 is weaker for more sustained agonist application (Weitlauf et al. 2005). Meanwhile, the partial NR2B-NR blockade by NVP-AAM077 is unlikely to have been the cause of the abolition of potentiation because full NR2B-NR blockade with Ro25-6981 fails to do so. Furthermore, the final plasticity outcome for STDP (and perhaps classical LTP/LTD) is likely determined by the competition among NMDAR-subtype–dependent signaling modules rather than by the absolute activation of a particular module (or related receptor subtype). Therefore although pharmacological separation of NMDAR subtypes is imperfect, differential inhibition of subtypes could have a decisive effect by biasing such competition (Li et al. 2006; Mallon et al. 2005).

Our CV analyses indicate that for a subpopulation of synapses, spike-timing-dependent LTD is presynaptically expressed, in consonance with the findings at cortical synapses (Bender et al. 2006; Sjostrom et al. 2003). However, this LTD apparently did not require a CB1 receptor signaling pathway, in contrast to what was previously observed in the neocortex (Bender et al. 2006; Sjostrom et al. 2003). One possibility is that other cannabinoid receptors such as the AM-251–insensitive CBsc receptor (Hajos et al. 2001) play an important role in the control of glutamatergic transmission in the hippocampus (Hoffman et al. 2005). Despite this evidence for the presynaptic expression of LTD, our model contains an implicit assumption that the signaling modules *P*, *D*, and *V* all reside in the postsynaptic compartment where they interact with one another as well as upstream and downstream signaling factors. This assumption is favorable because these modules must be able to discriminate between stimuli with millisecond precision to achieve the correct plasticity outcome. In such a picture, presynaptic expression of LTD would occur only after the completion of an upstream computation occurring entirely in the postsynaptic compartment. Under certain conditions (e.g., *BA*), completion of this computation through dynamic interaction among postsynaptic signaling modules could result in the production of a retrograde messenger, which in turn would induce the expression of LTD at a presynaptic locus.

However, recent studies revealed possibilities for presynaptic coincidence detection in the induction of certain types of synaptic plasticity, including spike-timing-dependent depression in the neocortex involving retrograde endocannabinoid signaling and activation of putatively presynaptic NR2B-NRs (Duguid and Sjostrom 2006). If similar mechanisms exist in hippocampal neurons, an attractive alternative to purely postsynaptic modules would be a framework in which postsynaptic NR2A-NRs linked to postsynaptic *P*, working with presynaptic NR2B-NRs linked to presynaptic *D*. In fact, the general features of our model of modular competition are also compatible with this picture, as long as *V* resides in the same compartment with *D*, arising from kinetic considerations. Unfortunately, we were unable to directly test this idea because manipulations such as selective blockade of presynaptic NR2B-NRs are difficult to attain under perforated patch-clamp conditions.

There are several potential mechanisms by which NMDAR subtypes could selectively activate different modules. One possibility is the differential localization of the two subtypes on pre- and postsynaptic compartments, as discussed earlier. For the alternative hypothesis of all-postsynaptic modules, it was previously suggested that the subcellular localization (e.g., synaptic vs. extrasynaptic) of NR2A- and NR2B-NRs could

confer on them differential sensitivity to contrasting stimulus patterns (Bliss and Schoepfer 2004). Differential subcellular localization could also lead to different spatiotemporal patterns of calcium influx and intrasynaptic diffusion, thus preferentially activating different modules. At a finer scale, specific macromolecular assemblies (Kennedy et al. 2005) responsible for activating potentiation or depression could be directly coupled to synaptic NR2A- and NR2B-NRs, respectively (Kim et al. 2005; Li et al. 2006; Tigaret et al. 2006). In such cases, Ca^{2+} transients at "microdomains" (Blackstone and Sheng 2002) may directly activate such molecular modules, including those involving CaMKII or CaN, leading to structural and functional changes at synapses.

Because activated CaMKII localizes to NR2B-NRs, their interaction is likely to be important for LTP expression (Barria and Malinow 2005; Bayer et al. 2001). Yet the roles of NMDAR subtypes and CaMKII in scaffolding may be quite distinct from their roles in signaling. Because NR2A-NRs undergo more rapid relief of Mg^{2+} block by back-propagating action potentials (Clarke and Johnson 2005), and have a fourfold higher peak open probability than that of NR2B-NRs (Chen et al. 1999; Erreger et al. 2005), NR2A-NRs may permit significantly greater Ca^{2+} influx during STDP-associated excitatory postsynaptic potential–spike interactions than do NR2B-NRs (Kampa et al. 2004). Thus NR2A-NRs may be necessary to activate a (soluble) pool of inactive CaMKII. The activated CaMKII could then bind to NR2B-NRs and recruit AMPARs for the expression of LTP (Lisman et al. 2002). The signal/scaffold model also puts NR2B-NRs in a prime position to mediate LTD because phosphatases activated by Ca^{2+} influx through NR2B-NRs would be optimally located to disrupt this assembly. Nonetheless, in certain brain areas, at certain developmental ages, or under certain genetic manipulations, LTP may in part be signaled by non-NR2A NMDAR subtypes (Barria and Malinow 2005; Berberich et al. 2005; Weitlauf et al. 2005; Zhao et al. 2005). Whether a different kind of NMDAR subtype specificity for STDP exists under such conditions remains to be investigated.

Finally, because of the striking difference in the kinetics of NR2A- and NR2B-NRs, it is also possible that the kinetics itself is responsible for subtype-specific activation of STDP modules. Previous attempts to explain differential roles for NMDAR subtypes based on kinetics (Erreger et al. 2005) relied on differences in the stimulation frequency used to evoke LTP compared with LTD. However, in STDP potentiation and depression are achieved at the same stimulus frequency. Thus a different mechanism is needed for a kinetic model to explain STDP. Indeed, a model using postsynaptic Ca^{2+} dynamics was able to recapitulate the results from previous spike multiplet experiments, as were conventional protocols for the induction of synaptic plasticity (Rubin et al. 2005). The difference in NMDAR-mediated current kinetics between those that we observed in the presence of NVP-AAM077 and those in the presence of Ro25-6981 (Fig. 1) may provide further evidence that slow Ca^{2+} transients are better for depression and fast Ca^{2+} transients are better for potentiation (Zhou et al. 2005). Interestingly, differences in receptor kinetics, subcellular localization, and potential macromolecular assemblies could all favor the same discrimination—thus it is possible that they work in parallel to ensure reliable modular competition in NMDAR-dependent synaptic plasticity.

ACKNOWLEDGMENTS

Special thanks to A. L. Barth and N. N. Urban for comments on the manuscript. We thank Dr. Y. P. Auberson at Novartis Pharma AG, Basel for the generous gift of NVP-AAM077.

GRANTS

This work was partially supported by Burroughs Wellcome Fund (Career Award in the Biomedical Sciences) and National Institute of Mental Health (NIMH) Grant R01 MH-066962 to G.-Q. Bi. R. C. Gerkin was a recipient of Integrative Graduate Education and Research Traineeship Fellowship DGE-9987588 from the National Science Foundation and a National Research Service/NIMH Award F31 MH-077430.

REFERENCES

Abbott LF, Nelson SB. Synaptic plasticity: taming the beast. *Nat Neurosci Suppl* 3: 1178–1183, 2000.

Artola A, Singer W. Long-term depression of excitatory synaptic transmission and its relationship to long-term potentiation. *Trends Neurosci* 16: 480–487, 1993.

Bagal AA, Kao JP, Tang CM, Thompson SM. Long-term potentiation of exogenous glutamate responses at single dendritic spines. *Proc Natl Acad Sci USA* 102: 14434–14439, 2005.

Barria A, Malinow R. NMDA receptor subunit composition controls synaptic plasticity by regulating binding to CaMKII. *Neuron* 48: 289–301, 2005.

Bayer KU, De Koninck P, Leonard AS, Hell JW, Schulman H. Interaction with the NMDA receptor locks CaMKII in an active conformation. *Nature* 411: 801–805, 2001.

Bender VA, Bender KJ, Brasier DJ, Feldman DE. Two coincidence detectors for spike timing-dependent plasticity in somatosensory cortex. *J Neurosci* 26: 4166–4177, 2006.

Berberich S, Punnakkal P, Jensen V, Pawlak V, Seeburg PH, Hvalby O, Kohr G. Lack of NMDA receptor subtype selectivity for hippocampal long-term potentiation. *J Neurosci* 25: 6907–6910, 2005.

Bi GQ, Poo MM. Synaptic modifications in cultured hippocampal neurons: dependence on spike timing, synaptic strength, and postsynaptic cell type. *J Neurosci* 18: 10464–10472, 1998.

Bi GQ, Poo MM. Synaptic modification by correlated activity: Hebb's postulate revisited. *Annu Rev Neurosci* 24: 139–166, 2001.

Bi GQ, Rubin JE. Timing in synaptic plasticity: from detection to integration. *Trends Neurosci* 28: 222–228, 2005.

Blackstone C, Sheng M. Postsynaptic calcium signaling microdomains in neurons. *Front Biosci* 7: d872–d885, 2002.

Bliss T, Schoepfer R. Neuroscience. Controlling the ups and downs of synaptic strength. *Science* 304: 973–974, 2004.

Bliss TV, Collingridge GL. A synaptic model of memory: long-term potentiation in the hippocampus. *Nature* 361: 31–39, 1993.

Bradshaw JM, Kubota Y, Meyer T, Schulman H. An ultrasensitive Ca^{2+}/calmodulin-dependent protein kinase II-protein phosphatase 1 switch facilitates specificity in postsynaptic calcium signaling. *Proc Natl Acad Sci USA* 100: 10512–10517, 2003.

Brimecombe JC, Boeckman FA, Aizenman E. Functional consequences of NR2 subunit composition in single recombinant N-methyl-D-aspartate receptors. *Proc Natl Acad Sci USA* 94: 11019–11024, 1997.

Cai Y, Gavornik JP, Cooper LN, Yeung LC, Shouval HZ. Effect of stochastic synaptic and dendritic dynamics on synaptic plasticity in visual cortex and hippocampus. *J Neurophysiol* 97: 375–386, 2006.

Chen N, Luo T, Raymond LA. Subtype-dependence of NMDA receptor channel open probability. *J Neurosci* 19: 6844–6854, 1999.

Clarke R, Johnson J. Voltage-dependent gating of NMDA receptors in the presence and absence of magnesium. *SFN Annual Meeting* 721.726, 2005.

Constantine-Paton M, Cline HT, Debski E. Patterned activity, synaptic convergence, and the NMDA receptor in developing visual pathways. *Annu Rev Neurosci* 13: 129–154, 1990.

Cull-Candy S, Brickley S, Farrant M. NMDA receptor subunits: diversity, development and disease. *Curr Opin Neurobiol* 11: 327–335, 2001.

Dan Y, Poo MM. Spike timing-dependent plasticity of neural circuits. *Neuron* 44: 23–30, 2004.

Duguid I, Sjostrom PJ. Novel presynaptic mechanisms for coincidence detection in synaptic plasticity. *Curr Opin Neurobiol* 16: 312–322, 2006.

Erreger K, Dravid SM, Banke TG, Wyllie DJ, Traynelis SF. Subunit-specific gating controls rat NR1/NR2A and NR1/NR2B NMDA channel kinetics and synaptic signalling profiles. *J Physiol* 563: 345–358, 2005.

Faber DS, Korn H. Applicability of the coefficient of variation method for analyzing synaptic plasticity. *Biophys J* 60: 1288–1294, 1991.

Feng B, Tse HW, Skifter DA, Morley R, Jane DE, Monaghan DT. Structure-activity analysis of a novel NR2C/NR2D-preferring NMDA receptor antagonist: 1-(phenanthrene-2-carbonyl) piperazine-2,3-dicarboxylic acid. *Br J Pharmacol* 141: 508–516, 2004.

Fischer G, Mutel V, Trube G, Malherbe P, Kew JN, Mohacsi E, Heitz MP, Kemp JA. Ro 25–6981, a highly potent and selective blocker of N-methyl-D-aspartate receptors containing the NR2B subunit. Characterization in vitro. *J Pharmacol Exp Ther* 283: 1285–1292, 1997.

Froemke RC, Dan Y. Spike-timing-dependent synaptic modification induced by natural spike trains. *Nature* 416: 433–438, 2002.

Hajos N, Ledent C, Freund TF. Novel cannabinoid-sensitive receptor mediates inhibition of glutamatergic synaptic transmission in the hippocampus. *Neuroscience* 106: 1–4, 2001.

Hatton CJ, Paoletti P. Modulation of triheteromeric NMDA receptors by N-terminal domain ligands. *Neuron* 46: 261–274, 2005.

Hebb DO. *The Organization of Behavior.* New York: Wiley, 1949.

Hoffman AF, Macgill AM, Smith D, Oz M, Lupica CR. Species and strain differences in the expression of a novel glutamate-modulating cannabinoid receptor in the rodent hippocampus. *Eur J Neurosci* 22: 2387–2391, 2005.

Janssens N, Lesage AS. Glutamate receptor subunit expression in primary neuronal and secondary glial cultures. *J Neurochem* 77: 1457–1474, 2001.

Kampa BM, Clements J, Jonas P, Stuart GJ. Kinetics of Mg^{2+} unblock of NMDA receptors: implications for spike-timing dependent synaptic plasticity. *J Physiol* 556: 337–345, 2004.

Kennedy MB, Beale HC, Carlisle HJ, Washburn LR. Integration of biochemical signalling in spines. *Nat Rev Neurosci* 6: 423–434, 2005.

Kew JN, Richards JG, Mutel V, Kemp JA. Developmental changes in NMDA receptor glycine affinity and ifenprodil sensitivity reveal three distinct populations of NMDA receptors in individual rat cortical neurons. *J Neurosci* 18: 1935–1943, 1998.

Kim MJ, Dunah AW, Wang YT, Sheng M. Differential roles of NR2A- and NR2B-containing NMDA receptors in Ras-ERK signaling and AMPA receptor trafficking. *Neuron* 46: 745–760, 2005.

Kuner T, Schoepfer R. Multiple structural elements determine subunit specificity of Mg^{2+} block in NMDA receptor channels. *J Neurosci* 16: 3549–3558, 1996.

Kutsuwada T, Kashiwabuchi N, Mori H, Sakimura K, Kushiya E, Araki K, Meguro H, Masaki H, Kumanishi T, Arakawa M, Mishina M. Molecular diversity of the NMDA receptor channel. *Nature* 358: 36–41, 1992.

Lester RA, Quarum ML, Parker JD, Weber E, Jahr CE. Interaction of 6-cyano-7-nitroquinoxaline-2,3-dione with the *N*-methyl-D-aspartate receptor-associated glycine binding site. *Mol Pharmacol* 35: 565–570, 1989.

Li S, Tian X, Hartley D, Feig L. Distinct roles for Ras-guanine nucleotide-releasing factor 1 (Ras-GRF1) and Ras-GRF2 in the induction of long-term potentiation and long-term depression. *J Neurosci* 26: 1721–1729, 2006.

Lisman J. A mechanism for the Hebb and the anti-Hebb processes underlying learning and memory. *Proc Natl Acad Sci USA* 86: 9574–9578, 1989.

Lisman J, Schulman H, Cline H. The molecular basis of CaMKII function in synaptic and behavioural memory. *Nat Rev Neurosci* 3: 175–190, 2002.

Liu L, Wong TP, Pozza MF, Lingenhoehl K, Wang Y, Sheng M, Auberson YP, Wang YT. Role of NMDA receptor subtypes in governing the direction of hippocampal synaptic plasticity. *Science* 304: 1021–1024, 2004.

Malenka RC, Nicoll RA. Long-term potentiation—a decade of progress. *Science* 285: 1870–1874, 1999.

Mallon AP, Auberson YP, Stone TW. Selective subunit antagonists suggest an inhibitory relationship between NR2B and NR2A-subunit containing N-methyl-D-aspartate receptors in hippocampal slices. *Exp Brain Res* 162: 374–383, 2005.

Massey PV, Johnson BE, Moult PR, Auberson YP, Brown MW, Molnar E, Collingridge GL, Bashir ZI. Differential roles of NR2A- and NR2B-containing NMDA receptors in cortical long-term potentiation and long-term depression. *J Neurosci* 24: 7821–7828, 2004.

Miyashiro K, Dichter M, Eberwine J. On the nature and differential distribution of mRNAs in hippocampal neurites: implications for neuronal functioning. *Proc Natl Acad Sci USA* 91: 10800–10804, 1994.

Monyer H, Burnashev N, Laurie DJ, Sakmann B, Seeburg PH. Developmental and regional expression in the rat brain and functional properties of four NMDA receptors. *Neuron* 12: 529–540, 1994.

Morishita W, Lu W, Smith GB, Nicoll RA, Bear MF, Malenka RC. Activation of NR2B-containing NMDA receptors is not required for NMDA receptor-dependent long-term depression. *Neuropharmacology* 52: 71–76, 2007.

Nevian T, Sakmann B. Single spine Ca^{2+} signals evoked by coincident EPSPs and backpropagating action potentials in spiny stellate cells of layer 4 in the juvenile rat somatosensory barrel cortex. *J Neurosci* 24: 1689–1699, 2004.

Nevian T, Sakmann B. Spine Ca^{2+} signaling in spike-timing-dependent plasticity. *J Neurosci* 26: 11001–11013, 2006.

Neyton J, Paoletti P. Relating NMDA receptor function to receptor subunit composition: limitations of the pharmacological approach. *J Neurosci* 26: 1331–1333, 2006.

Noceti F, Baldelli P, Wei X, Qin N, Toro L, Birnbaumer L, Stefani E. Effective gating charges per channel in voltage-dependent K^+ and Ca^{2+} channels. *J Gen Physiol* 108: 143–155, 1996.

Okada M, Corfas G. Neuregulin1 downregulates postsynaptic GABAA receptors at the hippocampal inhibitory synapse. *Hippocampus* 14: 337–344, 2004.

Palmer MJ, Isaac JT, Collingridge GL. Multiple, developmentally regulated expression mechanisms of long-term potentiation at CA1 synapses. *J Neurosci* 24: 4903–4911, 2004.

Rubin JE, Gerkin RC, Bi GQ, Chow CC. Calcium time course as a signal for spike-timing-dependent plasticity. *J Neurophysiol* 93: 2600–2613, 2005.

Shouval HZ, Bear MF, Cooper LN. A unified model of NMDA receptor-dependent bidirectional synaptic plasticity. *Proc Natl Acad Sci USA* 99: 10831–10836, 2002.

Shouval HZ, Kalantzis G. Stochastic properties of synaptic transmission affect the shape of spike time-dependent plasticity curves. *J Neurophysiol* 93: 1069–1073, 2005.

Sjostrom PJ, Nelson SB. Spike timing, calcium signals and synaptic plasticity. *Curr Opin Neurobiol* 12: 305–314, 2002.

Sjostrom PJ, Turrigiano GG, Nelson SB. Rate, timing, and cooperativity jointly determine cortical synaptic plasticity. *Neuron* 32: 1149–1164, 2001.

Sjostrom PJ, Turrigiano GG, Nelson SB. Neocortical LTD via coincident activation of presynaptic NMDA and cannabinoid receptors. *Neuron* 39: 641–654, 2003.

Stemmer PM, Klee CB. Dual calcium ion regulation of calcineurin by calmodulin and calcineurin B. *Biochemistry* 33: 6859–6866, 1994.

Tang YP, Shimizu E, Dube GR, Rampon C, Kerchner GA, Zhuo M, Liu G, Tsien JZ. Genetic enhancement of learning and memory in mice. *Nature* 401: 63–69, 1999.

Tigaret CM, Thalhammer A, Rast GF, Specht CG, Auberson YP, Stewart MG, Schoepfer R. Subunit dependencies of *N*-methyl-D-aspartate (NMDA) receptor-induced alpha-amino-3-hydroxy-5-methyl-4-isoxazolepropionic acid (AMPA) receptor internalization. *Mol Pharmacol* 69: 1251–1259, 2006.

Vicini S, Wang JF, Li JH, Zhu WJ, Wang YH, Luo JH, Wolfe BB, Grayson DR. Functional and pharmacological differences between recombinant *N*-methyl-D-aspartate receptors. *J Neurophysiol* 79: 555–566, 1998.

Wang HX, Gerkin RC, Nauen DW, Bi GQ. Coactivation and timing-dependent integration of synaptic potentiation and depression. *Nat Neurosci* 8: 187–193, 2005.

Weitlauf C, Honse Y, Auberson YP, Mishina M, Lovinger DM, Winder DG. Activation of NR2A-containing NMDA receptors is not obligatory for NMDA receptor-dependent long-term potentiation. *J Neurosci* 25: 8386–8390, 2005.

Wilcox KS, Buchhalter J, Dichter MA. Properties of inhibitory and excitatory synapses between hippocampal neurons in very low density cultures. *Synapse* 18: 128–151, 1994.

Yang SN, Tang YG, Zucker RS. Selective induction of LTP and LTD by postsynaptic $[Ca^{2+}]_i$ elevation. *J Neurophysiol* 81: 781–787, 1999.

Yang Y, Ge W, Chen Y, Zhang Z, Shen W, Wu C, Poo M, Duan S. Contribution of astrocytes to hippocampal long-term potentiation through release of D-serine. *Proc Natl Acad Sci USA* 100: 15194–15199, 2003.

Zhao MG, Toyoda H, Lee YS, Wu LJ, Ko SW, Zhang XH, Jia Y, Shum F, Xu H, Li BM, Kaang BK, Zhuo M. Roles of NMDA NR2B subtype receptor in prefrontal long-term potentiation and contextual fear memory. *Neuron* 47: 859–872, 2005.

Zhou YD, Acker CD, Netoff TI, Sen K, White JA. Increasing Ca^{2+} transients by broadening postsynaptic action potentials enhances timing-dependent synaptic depression. *Proc Natl Acad Sci USA* 102: 19121–19125, 2005.